Electronic Supplementary Material (ESI) for Journal of Materials Chemistry A.

Supplementary Information

Fatigue Resistance of a Flexible, Efficient, and Metal Oxide-Free Perovskite Solar Cell

Kianoosh Poorkazem, Dianyi Liu and Timothy L. Kelly*

Department of Chemistry, University of Saskatchewan
110 Science Place, Saskatoon, SK, Canada, S7N 5C9

* e-mail: tim.kelly@usask.ca

Experimental

Materials

0.25 mm thick PET, 0.2 mm thick M-In_2O_3-coated PET ($R_s \leq 10$ Ω/□), and 0.15 mm thick ITO-coated PET ($R_s = 60$ Ω/□) substrates were purchased from McMaster-Carr, Delta Technologies, and Sigma-Aldrich, respectively. HC-PEDOT and SC-PEDOT were purchased from Clevios (PH1000 and P VP AI 4083, respectively). Zonyl F-300 fluorosurfactant (40% solids in H_2O) was purchased from Fluka. ZnO nanoparticle[1] and CH_3NH_3I[2] solutions was synthesized according to literature procedures. Zinc acetate dihydrate, methylamine solution (33% in ethanol), hydriodic acid, lead(II) iodide, 4-*tert*-butylpyridine, and lithium bis(trifluoromethylsulphonyl)imide were purchased from Sigma-Aldrich, Alfa Aesar or Fisher Scientific. Spiro-OMeTAD was purchased from Merck KGaA. $PC_{61}BM$ was purchased from Nano-C, and P3HT was purchased from Rieke Metals, Inc.

Methods

M-In_2O_3/ZnO/$CH_3NH_3PbI_3$ Device Fabrication. This process was adapted from literature procedures.[1] A 3 mg/mL ZnO nanoparticle solution was prepared in butanol containing 6.25% (v/v) methanol and 6.25% (v/v) chloroform. Three layers of ZnO nanoparticles were deposited on the PET/M-In_2O_3 substrate via sequential spin-coating steps (3000 rpm for 30 s). The ZnO layer was allowed to dry for at least 0.5 h. A solution of 460 mg/mL PbI_2 in DMF was prepared and heated to 100 ^oC, and used to deposit a PbI_2 thin film by spin coating (3000 rpm for 20-25 s). The PbI_2 layer was allowed to dry for 1 h. Afterward, the samples were immersed in a solution of 10 mg/mL CH_3NH_3I in dry isopropanol for 60 s and then spin-dried immediately at 2000 rpm for 10 s. Spiro-OMeTAD was deposited by spin-coating (4000 rpm for 30 s) from a solution of 80 mg spiro-OMeTAD, 28.5 μL 4-*tert*-butylpyridine and 17.5 μL lithium-bis(trifluoromethanesulfonyl)imide (Li-TFSI) solution (520 mg Li-TFSI in 1 mL acetonitrile) all dissolved in 1 mL chlorobenzene. Ag counter-electrodes (150 nm) were deposited by thermal evaporation at a base pressure of 2×10^{-6} mbar at a rate of 0.1 Å/s for the first 15 nm and at a rate of 0.3 Å/s for another 135 nm.

HC-PEDOT/SC-PEDOT/P3HT:$PC_{61}BM$ Device Fabrication. The PET/HC-PEDOT/SC-PEDOT layers were fabricated as in the main text and allowed to cool to room temperature. The P3HT:$PC_{61}BM$ active layer was spin-coated (1000 rpm for 30 s) from a solution of 15 mg/mL P3HT and 12 mg/mL $PC_{61}BM$ in chlorobenzene (the solution was stirred for at least 2 h prior to deposition). The samples were then thermally annealed at 120 ^oC for 20 min. A 6 mg/mL solution of ZnO nanoparticles (in the

same solvent mixture as above) was spin-coated onto the active layer (1000 rpm for 30 s, followed by 3000 rpm for 10 s). Evaporation of Al electrodes was carried out as in the main text.

M-In_2O_3/ZnO/P3HT:$PC_{61}BM$ Device Fabrication. The PET/M-In_2O_3/ZnO layers were prepared as described above. The P3HT:$PC_{61}BM$ active layer was spin-coated (1000 rpm for 30 s) from a solution of 15 mg/mL P3HT and 12 mg/mL $PC_{61}BM$ in chlorobenzene (the solution was stirred for at least 2 h prior to deposition). After annealing at 120 ˚C for 15 min, a SC-PEDOT layer was deposited by spin-coating (4000 rpm for 60 s) and then further annealed at 120 ^{o}C for 15 min. For these devices, all spin-coating procedures were performed under ambient conditions, and all annealing steps were done inside the glovebox. Ag counter-electrodes (150 nm) were deposited as above.

Characterization

Absorption spectra were obtained using a Cary 6000i UV-vis-NIR spectrophotometer. Film thicknesses were measured using a KLA Tencor profilometer. IPCE spectra were acquired using a commercial setup (QE-PV-Si, Oriel Instruments) consisting of a 300 W Xe arc lamp, filter wheel, and monochromator. The incident light was chopped at a frequency of 30 Hz and photocurrents measured using a lock-in amplifier. Scanning electron microscopy images were acquired using a JEOL JSM-6010LV microscope at an accelerating voltage of 15 kV and a working distance of 11 mm. Powder X-ray diffraction patterns were obtained with a Bruker D8 Advance Series II diffractometer equipped with a Cu $K_{\alpha 1,2}$ X-ray source. The data were collected with a 0.0469° step size (2θ).

Figures and Tables

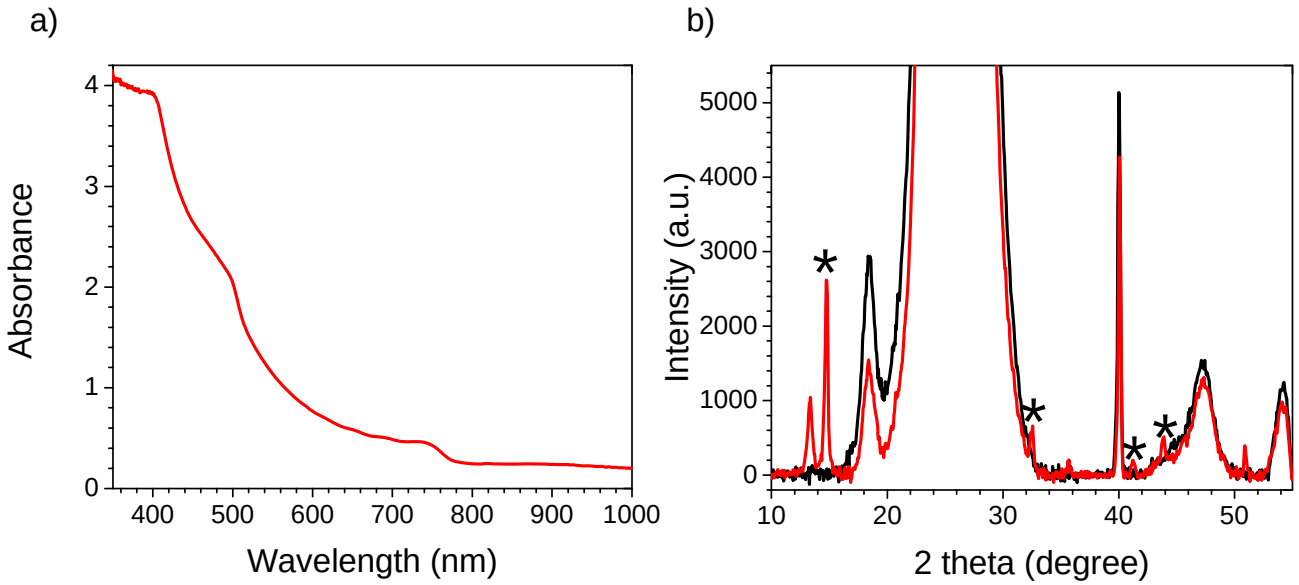

Figure S1. (a) Absorption spectrum and (b) pXRD pattern of PET/HC-PEDOT/SC-PEDOT/$CH_3NH_3PbI_3$ films (red lines). The pXRD pattern of the PET/HC-PEDOT/SC-PEDOT substrate (black line) is shown for comparison. Peaks marked with an asterisk (*) are due to the perovskite.

Table S1. Results of pairwise *t*-tests comparing the two PSCs at the 95% confidence level. Averages and standard deviations are calculated from 67 and 103 M-In_2O_3/ZnO/$CH_3NH_3PbI_3$ and HC-PEDOT/SC-PEDOT/$CH_3NH_3PbI_3$ devices, respectively. For each set of parameters, the critical *t*-value is 2.0.

Device Performance Parameters	**M-In_2O_3/ ZnO/$CH_3NH_3PbI_3$**	**HC-PEDOT/ SC-PEDOT/$CH_3NH_3PbI_3$**	***t*-statistic**	***p*-value**
V_{oc} (V)	0.90 ± 0.07	0.7 ± 0.2	12	1.2×10^{-24}
J_{sc} (mA/cm^2)	11 ± 2	11 ± 2	0.89	3.8×10^{-1}
FF	0.51 ± 0.07	0.5 ± 0.1	1.0	3.1×10^{-1}
PCE (%)	5 ± 2	4 ± 2	4.1	6.5×10^{-5}
R_s (ohm·cm^2)	(3 ± 1) × 10	17 ± 7	5.1	1.5×10^{-6}
R_{sh} (ohm·cm^2)	(5 ± 2) × 10^2	(1 ± 2) × 10^3	6.0	2.5×10^{-8}

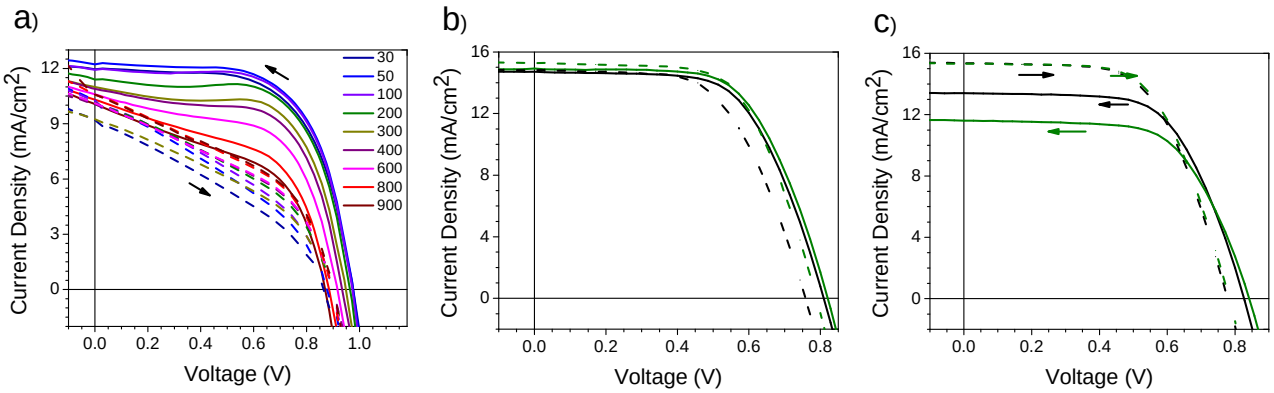

Figure S2. *J-V* curves of (a) M-In_2O_3/ZnO/$CH_3NH_3PbI_3$ devices, and HC-PEDOT/SC-PEDOT/$CH_3NH_3PbI_3$ devices at (b) short and (c) long dwell times. Scans from forward bias to short-circuit, and short-circuit to forward bias are shown as solid and dashed lines, respectively. In (a), the dwell time at each voltage step (in ms) is shown. In (b), dwell times were either 30 (black line) or 35 ms (green line). In (c), dwell times were either 100 (black line) or 200 ms (green line).

Table S2. Device performance parameters for P3HT:$PC_{61}BM$ solar cells. Averages and standard deviations are calculated from 66 devices of each type.

Electrode	V_{oc} (V)	J_{sc} (mA/cm^2)	FF	PCE (%)	R_s (Ω·cm^2)	R_{sh} (Ω·cm^2)
M-In_2O_3 (Average)	0.52 ± 0.08	6.6 ± 0.7	0.40 ± 0.06	1.4 ± 0.4	26 ± 9	(2.1 ± 0.7) × 10^2
M-In_2O_3 (Best)	0.58	7.3	0.50	2.1	14	3.5 × 10^2
HC-PEDOT (Average)	0.5 ± 0.1	6.4 ± 0.4	0.38 ± 0.06	1.2 ± 0.5	31 ± 7	(2.4 ± 1.3) × 10^2
HC-PEDOT (Best)	0.6	6.8	0.47	1.9	26	4.6 × 10^2

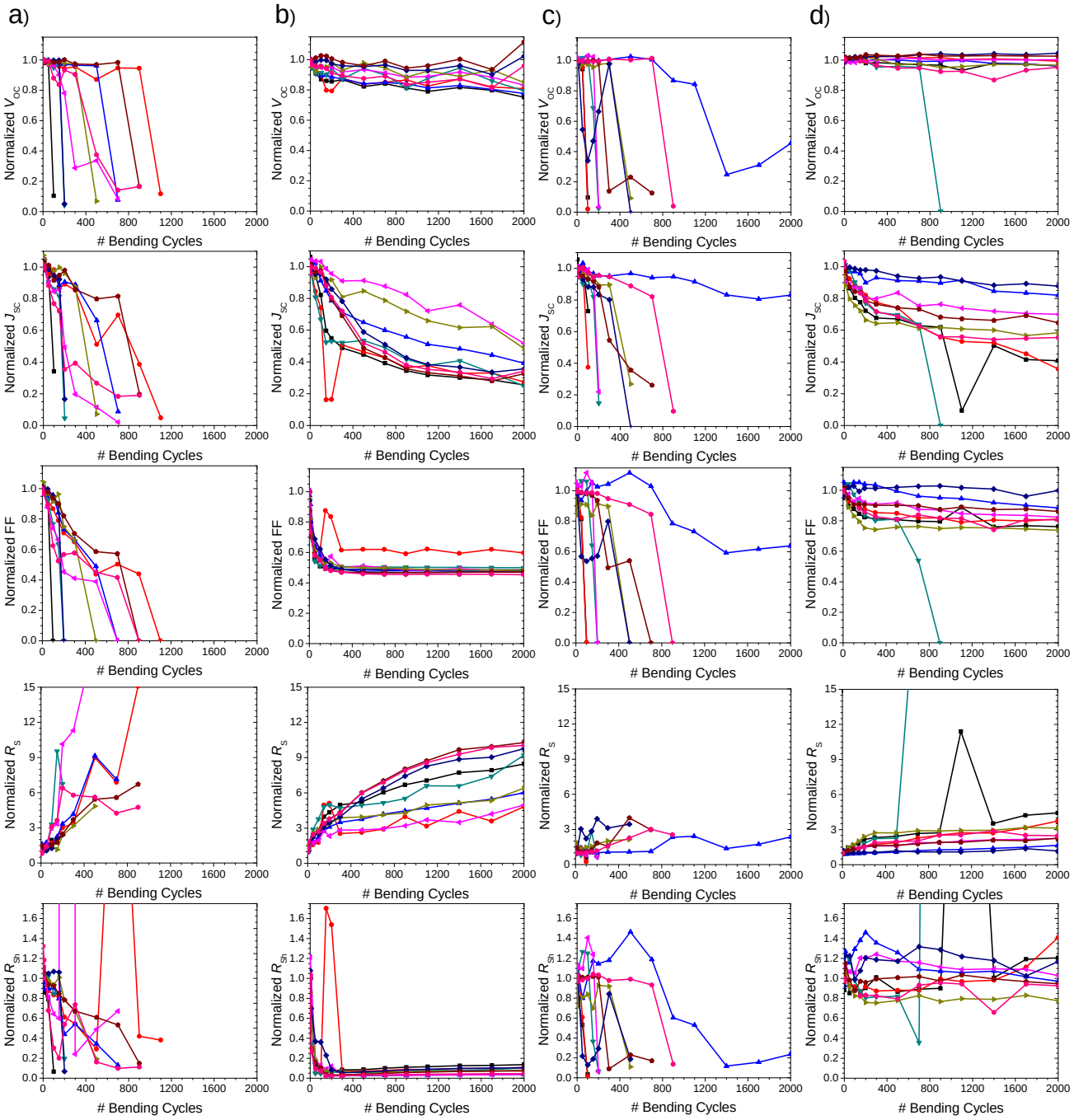

Figure S3. Results of the fatigue tests done on 9 separate devices (3 devices on each of 3 different substrates): (a) M-In_2O_3/ZnO/$CH_3NH_3PbI_3$, (b) HC-PEDOT/SC-PEDOT/$CH_3NH_3PbI_3$, (c) M-In_2O_3/ZnO/P3HT:$PC_{61}BM$, and (d) HC-PEDOT/SC-PEDOT/P3HT:$PC_{61}BM$. The rows (from top to bottom) show the normalized V_{oc} J_{sc}, FF, R_s, and R_{sh} values as a function of the number of bending cycles.

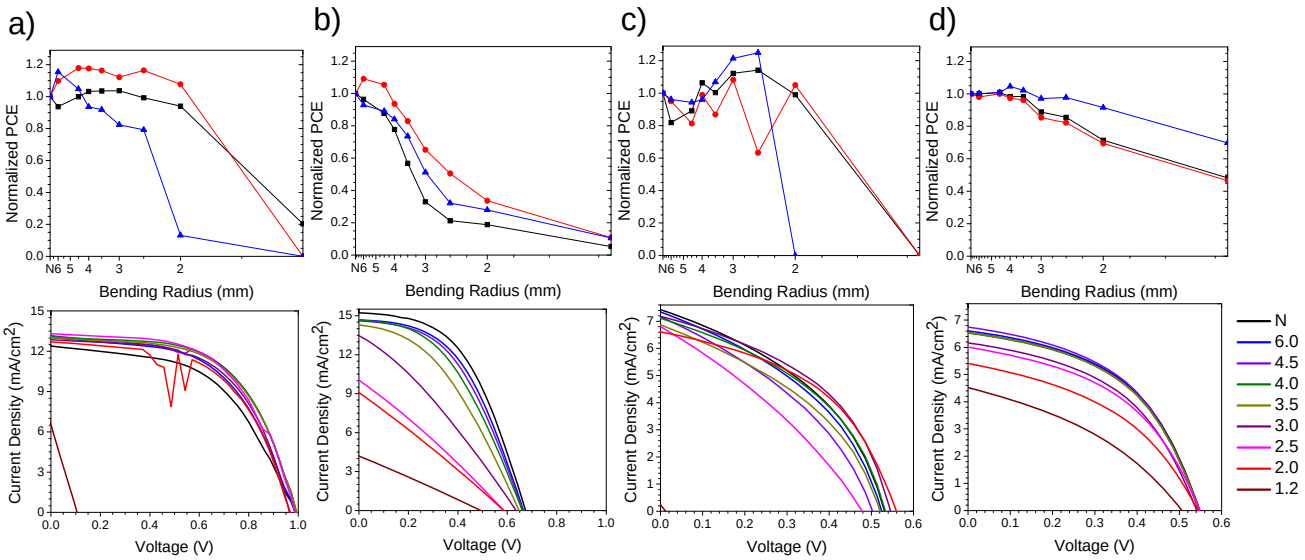

Figure S4. Results of the bending radius tests: (a) M-In_2O_3/ZnO/$CH_3NH_3PbI_3$, (b) HC-PEDOT/SC-PEDOT/$CH_3NH_3PbI_3$, (c) M-In_2O_3/ZnO/P3HT:$PC_{61}BM$, and (d) HC-PEDOT/SC-PEDOT/P3HT:$PC_{61}BM$. Devices were bent around cylindrical objects of varying radius, from the largest radius to the smallest. The initial performance is indicated by *N* (no bending). The top row shows the normalized PCE as a function of bending radius for each of 3 devices on a single substrate. The bottom row shows representative *J-V* curves as a function of the bending radius.

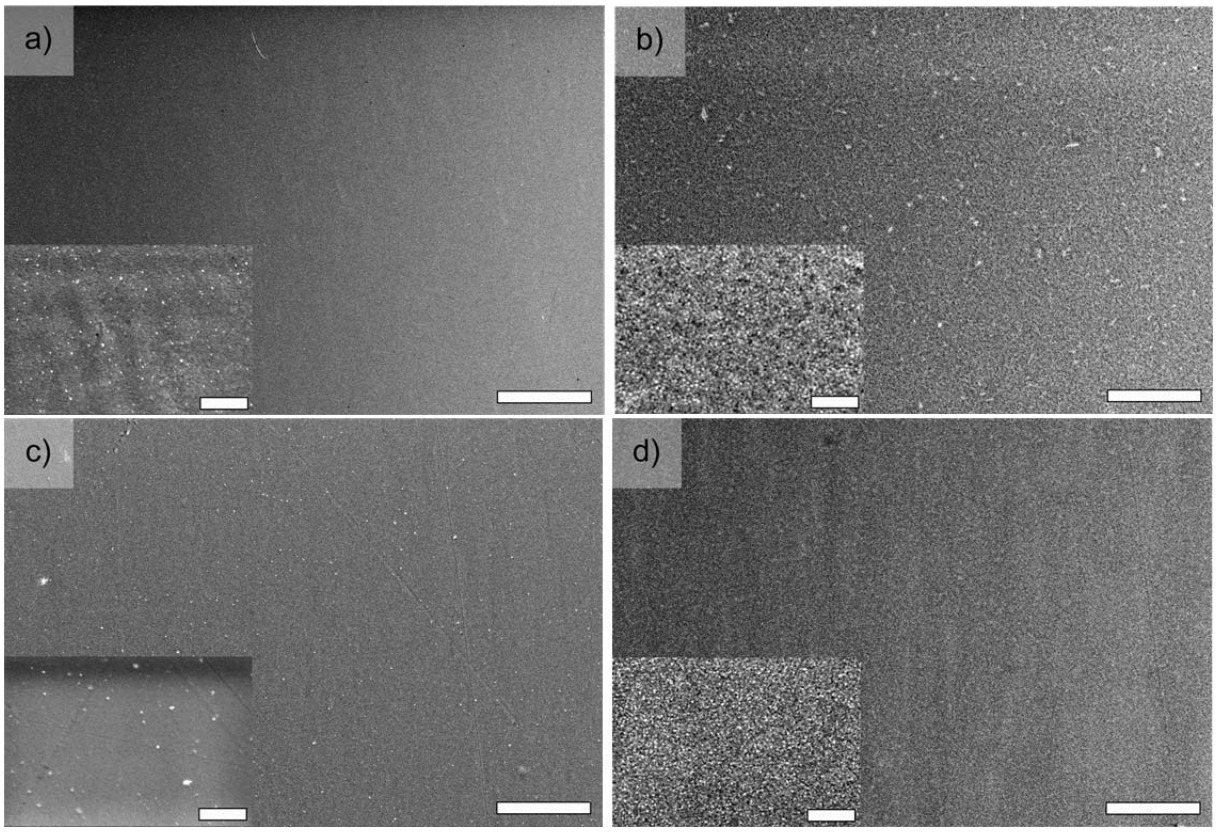

Figure S5. Low-magnification (main) and high-magnification (inset) SEM images of (a) PET/M-In_2O_3, (b) PET/M-In_2O_3/ZnO/$CH_3NH_3PbI_3$, (c) PET/HC-PEDOT, and (d) PET/HC-PEDOT/SC-PEDOT/$CH_3NH_3PbI_3$ films before bending. The scale bars in the main and inset images are 50 μm and 5 μm, respectively.

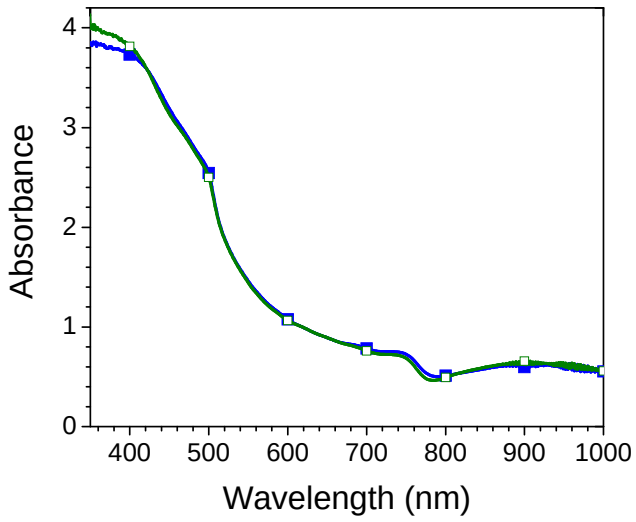

Figure S6. Absorption spectra of PET/M-In_2O_3/$CH_3NH_3PbI_3$ films before (solid blue squares) and after (open green squares) bending for 2000 cycles.

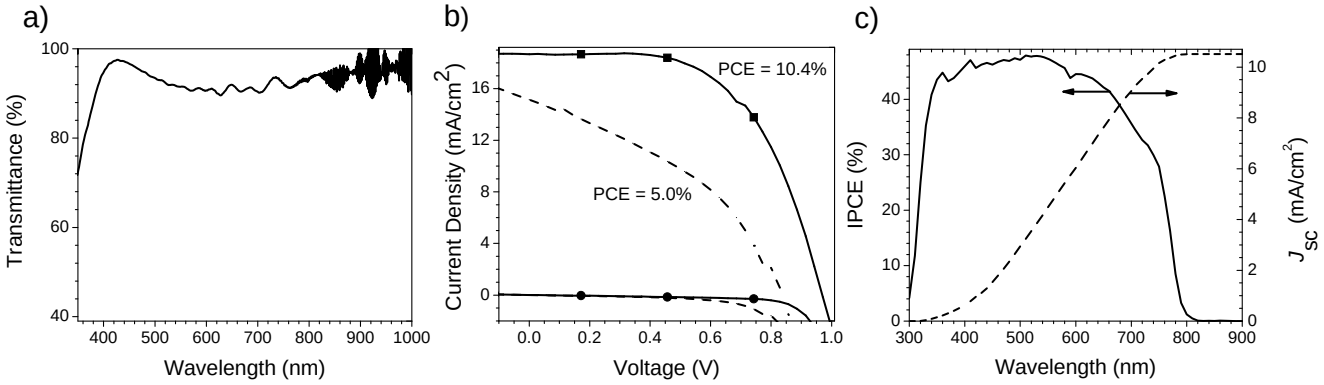

Figure S7. (a) Transmission spectrum of the ITO electrode, after subtraction of the PET background spectrum. (b) *J-V* curve of the ITO/ZnO/$CH_3NH_3PbI_3$/spiro-OMeTAD/Ag device, measured from forward bias to short-circuit (solid lines), and from short-circuit to forward bias (dashed lines), in both the light (squares) and in the dark (circles). (c) IPCE spectrum (solid line) and calculated J_{sc} value (dashed line) for a ITO/ZnO/$CH_3NH_3PbI_3$/spiro-OMeTAD/Ag device (the J_{sc} obtained from a reverse-scan *J-V* curve was 12 mA/cm^2).

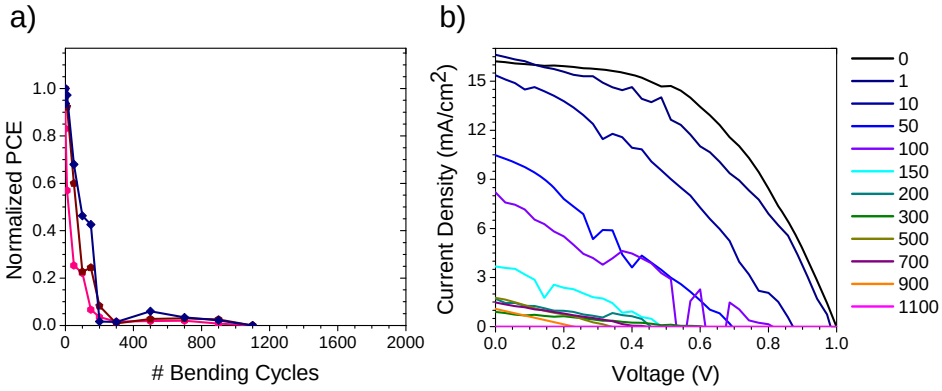

Figure S8. Results of the fatigue tests for ITO/ZnO/$CH_3NH_3PbI_3$/spiro-OMeTAD/Ag devices. (a) Normalized PCEs for 3 separate devices. (b) *J-V* curves as a function of the number of bending cycles for a typical device.

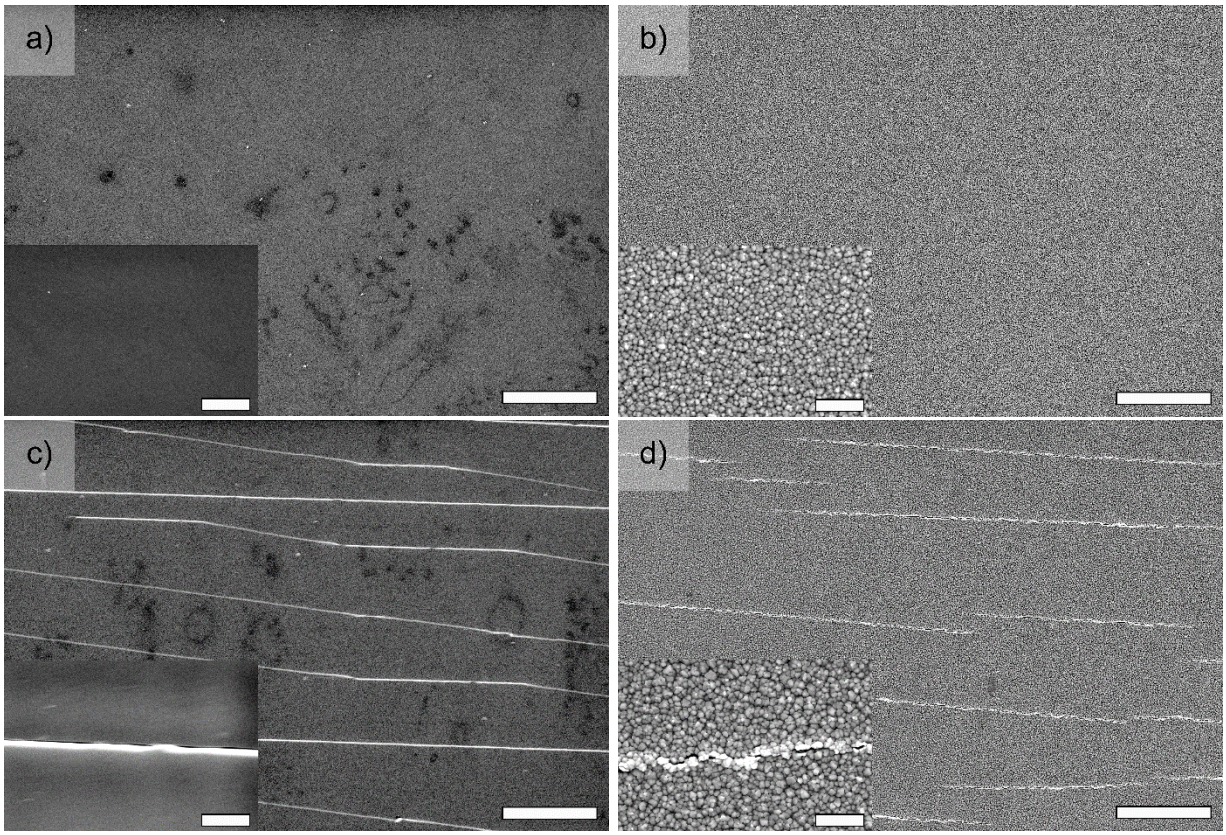

Figure S9. Low-magnification (main) and high-magnification (inset) SEM images of PET/ITO (a, c), and PET/ITO/ZnO/$CH_3NH_3PbI_3$ (b, d) films before (a, b) and after (c, d) 2200 bending cycles. The scale bars in the main and inset images are 50 μm and 5 μm, respectively.

References

1. D. Liu and T. L. Kelly, *Nat. Photonics.*, 2014, **8**, 133-138.
2. J. H. Im, C. R. Lee, J. W. Lee, S. W. Park and N. G. Park, *Nanoscale*, 2011, **3**, 4088-4093.